Article

A New Set of Isoreticular, Homochiral Metal-Organic Frameworks with UCP Topology

Michael Sartor, Timo Stein, Frank Hoffmann, and Michael Fröba

Chem. Mater., **Just Accepted Manuscript** • DOI: 10.1021/acs.chemmater.5b03723 • Publication Date (Web): 17 Dec 2015

A New Set of Isoreticular, Homochiral Metal-Organic Frameworks with ucp Topology

Michael Sartor, Timo Stein, Frank Hoffmann, and Michael Fröba*

Institute of Inorganic and Applied Chemistry, Department of Chemistry, University of Hamburg, Martin-Luther-King-Platz 6, D-20146 Hamburg, Germany

Metal-Organic Frameworks, Homochirality, Amino Acids, Enantioselective Catalysis

ABSTRACT: A new isoreticular series of metal–organic frameworks, called UHM-25 (UHM: University of Hamburg Materials), based on the copper paddle wheel motif and a novel set of homochiral linkers has been synthesized. Starting from amino acids available from the chiral pool a synthesis procedure was established that allows a straightforward, multi-gram scale synthesis of homochiral linkers in 4–5 steps. These linkers carry substituents that have been proven useful in stereoselective organic chemistry, such as the "Evans auxiliary" or chiral amino alcohols. The resulting MOFs only differ in the chiral moiety provided by the amino acid starting material. The structure of UHM-25 is composed of cuboctahedral cages of Cu_2 paddle wheel motifs connected by the isophthalate moieties of the linker. These cages are linked via the bent backbone of the linker resulting in a primitive cubic arrangement, giving rise to the underlying (3,4)-c binodal net **ucp**, which was hitherto only theoretically described. MOFs of the UHM-25 series show surface areas up to S_{BET} = 1900 m^2/g. Post-synthetic modification reactions with excellent conversion rates confirmed the accessibility to the chiral groups. Furthermore, UHM-25-Pro – bearing a prolinol functionality – was used in a self-directed, enantioselective aldol addition of acetaldehyde demonstrating the potential of the UHM-25 series with regard to heterogeneous, stereoselective catalysis.

INTRODUCTION

The inversion of the absolute configuration of a useful pharmaceutical and its metabolites can render them useless or even harmful, which has led regulatory authorities to impose producers of drugs on the requirement to provide stereochemically pure compounds, whenever possible.[1] Therefore, the preparation of enantiomerically pure compounds and the separation of racemic mixtures play important roles in the pharmaceutical industry. Solid-supported reagents that can provide so-called chiral information to substrates are highly interesting to pharmaceutical manufacturing.[2,3]

Metal-organic frameworks (MOFs) have gained substantial scientific interest over the last two decades and underwent an impressive development resulting in a wide variety of possible applications, in particular in the areas of gas storage,[4–8] separation[9–12] or catalytic applications.[13–17]

Homochiral MOFs may be eligible for uses in stereoselective processes.[18–21] They can provide a very high density of accessible functional groups that can serve for example as stereoselective transition metal catalysts.[22–28] Furthermore, the pore structure of MOFs may provide a chiral environment that accounts for stereoselectivity[29] and asymmetric reactions may benefit from rigid surroundings in the reaction step that defines the configuration of the stereocenter.[30]

To obtain homochiral MOFs, some approaches employ crystallization from chiral solvents[31,32] or in the presence of chiral additives[29,33–38] or they rely upon the addition of enantiopure auxiliary ligands to the inorganic building unit of the MOF.[39–46] Other approaches to synthesize chiral MOFs employ linker molecules with axial chirality[22,23,47–56] or precursor molecules that are obtained from chiral pool starting materials.[57–68]

Moreover, isoreticular approaches may be chosen by modifying a linker that has been established in other MOFs with enantiopure substituents, such as oxazolidinones[69] or pyrrolidines.[70,71] MOFs that include the latter may serve as asymmetric heterogeneous organocatalysts in which secondary amines represent the catalytically active site. These heterogeneous systems show great resemblance to proline-based organocatalysts and considerable stereochemical induction has been reported for these MOF-based systems.[30,70,71] However, in some cases only a general catalytic effect is documented[72] or a stereoselective catalysis is supposedly caused by adsorbed proline species released from the MOF,[73] which has been pointed out by Canivet and Farrusseng.[74] The proline-functionalized MOF DUT-32 in its Boc protected form was proven to be able to interact stereospecifically with *(S)-/(R)*-1-phenyl-2,2,2-trifluoroethanol that was used a chiral shift agent in solid-state NMR measurements, however, an asymmetric catalytic aldol test reaction with the deprotected DUT-32-NHPro MOF showed no specific stereoselectivity, probably because racemization occurred during the deprotection process.[71]

In the field of organocatalysis the proline motif has been improved by modifying the basic pyrrolidine structure with hydrogen donors and/or bulky substituents on the exocyclic carbon atom of the proline motif.[75,76] One example of this improvement is the α,α-diphenyl prolinol-system developed by Jørgenson and Hayashi.[76–78]

So far, a α,α-diaryl prolinol organocatalyst has not been included in a MOF.

Our approach to obtain homochiral MOFs uses molecules from the chiral pool as starting materials and transforms them into tetracarboxylic acid linkers. We chose amino acids for three reasons. First, they provide a carboxylic carbon atom that can serve as an electrophilic target for addition-elimination reactions. Second, numerous amino acids with a broad variety concerning their sterical properties and functional groups, are readily available in nature or can be easily synthesized.[79] Last, the nitrogen atom, inherent to amino acids, enables these compounds and their derivatives to act as stereoselective organocatalysts by providing a functional group that can bind substrates via enamine or imine bonds, thereby tethering the substrate in a chiral environment.[80,81] This is for example the case in reactions catalyzed by the α,α-diaryl prolinol system.

Here, we present a reaction pathway for new homochiral MOFs that employ diisophthalate linkers, which contain chiral amino acid substituents. This pathway yielded UHM-25, a new series of copper(II)-based, isoreticular MOFs. Materials from this UHM-25 series have been evaluated regarding their potential for post-synthetic modification (PSM) and enantioselective organocatalysis.

RESULTS AND DISCUSSION

Syntheses of the Linkers. A general approach to obtain the desired organic building units on a multi-gram scale was developed. The reagents from the chiral pool were modified to accommodate two aryl halides that offer the possibility of subsequent cross-coupling reactions to furnish tetracarboxylate linkers.

Based upon their individual molecular structure, the linker molecules used herein can be assigned to three types shown in Figure 1. Type 1 includes *N*-Boc (Boc: *tert*-butyloxycarbonyl) protected amino alcohol linkers, whereas type 2 comprises free amino alcohol linkers. Linker molecules featuring the Evans auxiliary motif are assigned to type 3. In the following, the reaction sequence for the synthesis of tetracarboxylic acid linkers starting from L-alanine is given. This procedure is representative for the preparation of the linkers used for preparation of the UHM-25 series. Detailed reaction schemes are given in the Supporting Information (SI).

Following Scheme 1, the carboxylic acid functional group of L-alanine was subjected to esterification and the amino group was subsequently protected with di-*tert*-butyl dicarbonate (Boc_2O) to give compound **2a**. An excess of 4-bromophenyllithium (prepared from 1,4-dibromobenzene and *n*-butyllithium) was reacted with the *N*-Boc protected methyl ester, resulting in the *N*-Boc protected amino alcohol **3a**.

In the next step, a Suzuki-Miyaura cross-coupling was performed between the α,α-diaryl amino alcohol **3a** and two equivalents of 3,5-di(methoxycarbonyl)phenylboronic acid. This reaction, shown in Scheme 2, provided the tetramethyl ester **4a**.

The tetramethyl ester **4a** was saponificated in a mixture of aqueous potassium hydroxide solution and tetrahydrofuran (THF). The reaction product was precipitated under mild acidic conditions. This furnished the first type of linker (**5a**) bearing an *N*-Boc protecting group. *N*-Boc groups can be cleaved thermolytically, thus releasing the free amine after the MOF synthesis.[70] This strategy can be used to prevent interpenetration[70] or may allow MOF syntheses where free amino groups would otherwise inhibit the formation of a framework.[71] Furthermore, the presence of a carbonyl group as a hydrogen bond acceptor may be beneficial for chiral recognition in MOFs.[82]

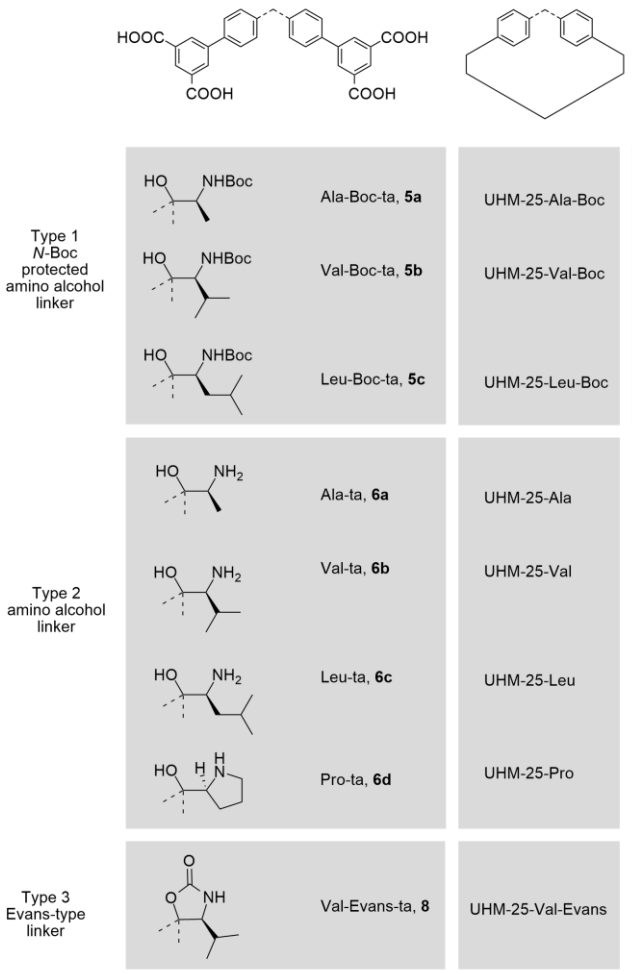

Figure 1. Overview of the different types of linkers used in the UHM-25 MOFs. Linkers and MOFs are named with the three-letter code of the respective amino acid used for the preparation of the linker, ta stands for tetracarboxylic acid. Boc appendix indicates the presence of the *N*-Boc protecting group (dashed lines mark the connection points to the framework host).

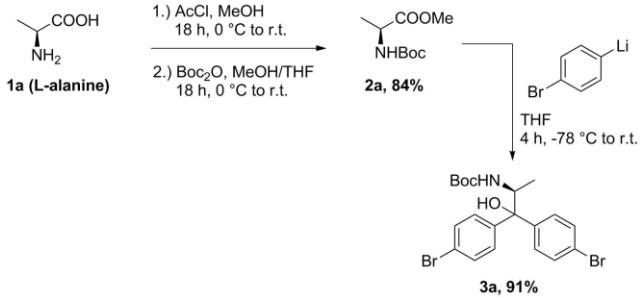

Scheme 1. Conversion of L-alanine to its protected derivative 2a and further reaction to the α,α-diaryl substituted, *N*-Boc protected tertiary amino alcohol 3a.

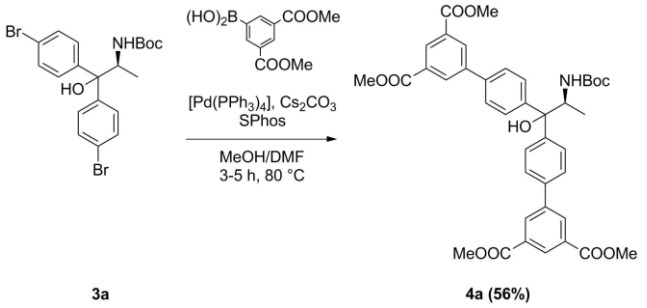

Scheme 2. Suzuki-Miyaura cross-coupling reaction of the *α,α*-di(4-bromophenyl) substituted, protected L-alaninol 3a to synthesize the tetramethyl ester of the linker molecule 4a.

To obtain the second type of linkers the *N*-Boc protected tetracarboxylic acids were deprotected using a mixture of trifluoroacetic acid (TFA) in dichloromethane according to Scheme 3. The resulting amine was precipitated as the corresponding TFA adduct **6a**. This salt was later used in the synthesis of a MOF without further purification.

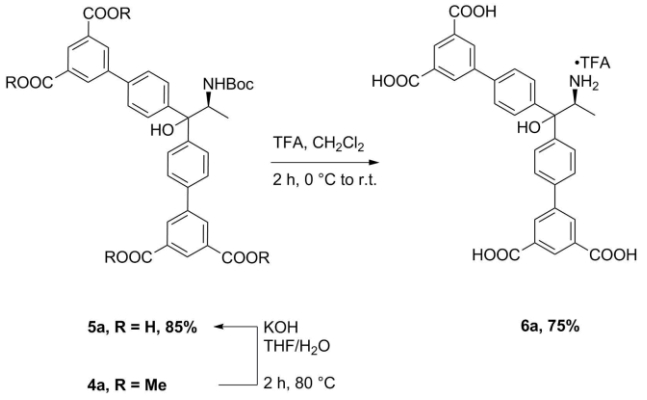

Scheme 3. Deprotection procedure for the primary amino alcohol 4a: First, tetramethyl esters were saponificated to give 5a, then the amino group was released acidolytically to yield 6a.

The linker bearing the Evans-type auxiliary constitutes the third type of linker (Evans-Val-ta). This type of linker was synthesized similar to the linkers described above (see SI for details).

Synthesis and Structure of the MOFs. In a typical synthesis of a UHM-25 series material, a solution of linker molecule in *N,N*-dimethylformamide (DMF) was acidified with nitric acid, an aqueous solution of copper(II) nitrate was added, and the reaction mixture was placed in a screw-capped flask in an oven for 72 h at 50 °C. This procedure furnished blue block-shaped crystals that were suitable for single-crystal X-ray diffraction experiments for UHM-25-Ala-Boc and UHM-25-Pro (further details on the determination of the crystal structure are given in the SI). MOFs were obtained as crystalline materials from each of the linkers depicted in Figure 1. Powder X-ray diffraction data of the MOFs shows phase purity and an isostructural relationship between the differently substituted MOFs (see Figure 2). To investigate and prove the stability of the chiral linkers after the MOF synthesis, the UHM-25 MOFs were digested in diluted hydrochloric acid. The integrity of the reisolated linkers was independently verified by ^{1}H NMR spectroscopy, mass spectrometry and optical rotation measurements.

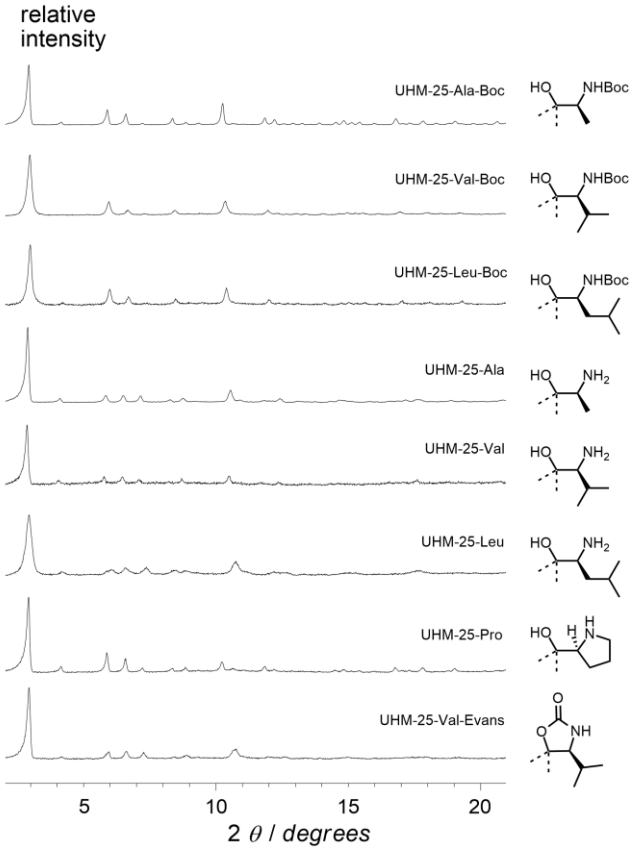

Figure 2. Powder X-ray diffractograms for all MOFs of the UHM-25 series. Structures of the chiral substituents are given next to the diffractograms (dashed lines mark the connection points to the framework host).

UHM-25-Ala-Boc crystallizes in the cubic space group *P*432 ($a = b = c = 28.9416$ Å). The tetracarboxylate linker serves as a 4-coordinated organic building unit. Copper paddle wheel motifs constitute square-planar inorganic secondary building units (SBUs). Due to the 120° angle between the carboxylate groups on the isophthalate moieties, cuboctahedral metal-organic polyhedra (MOP) with copper paddle wheel units being located at each corner are formed as subunits in this MOF.[83] These cuboctahedral MOP build a primitive cubic arrangement and each MOP is connected to every neighboring MOP via four linkers (see Figure 3).

Topological Considerations. Following the recommendations of O'Keeffe and Yaghi,[84] the branching points of the linker were explicitly included in the topological analysis. Accordingly, the inorganic SBU constitutes a square-planar 4-c node and the linker was considered as a set of two joint 3-c nodes instead as a single 4-c node. The topology of the UHM-25 MOF series was classified with the ToposPro suite.[85] The underlying topology of UHM-25 is the binodal (3,4)-c net **ucp**, which has been theoretically described as a possibility to connect cuboctahedral MOP by O'Keeffe and Yaghi[86] but has – to the best of our knowledge – not been found in a MOF so far.

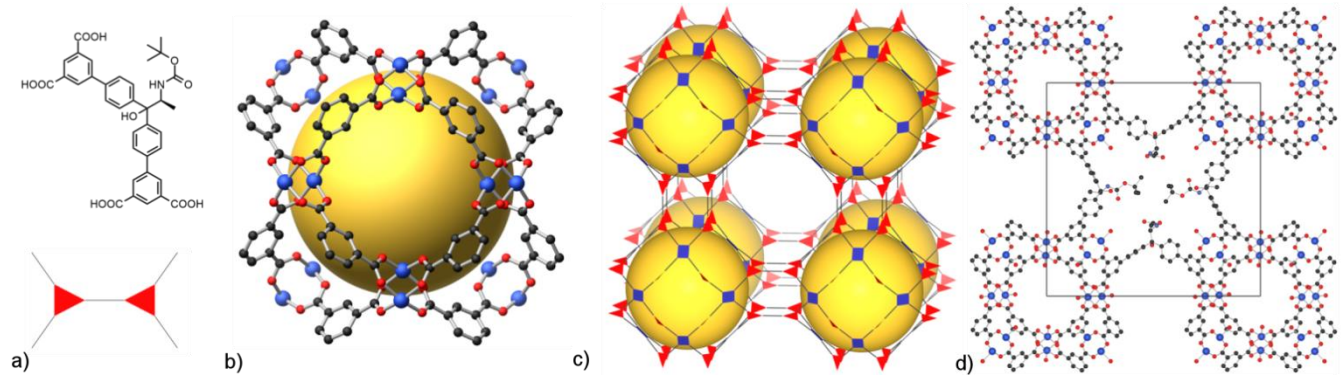

Figure 3. a) Representative linker Ala-Boc-ta used in the synthesis of UHM-25 MOFs and its topological representation as a set of two connected triangles, b) cuboctahedral MOP built from isophthalates and copper paddle wheels (the yellow sphere serves as a guide to the eye) c) cubic primitive arrangement of the cuboctahedral MOP giving rise to the (3,4)-c binodal net **ucp**, here shown in its augmented version **ucp-a**; d) view of the crystal structure of UHM-25-Ala-Boc along a crystallographic axis; the unit cell is indicated as a black square; for the linkers outside the unit cell only the isophthalate moieties are shown; hydrogen atoms as well as any disorder were omitted for clarity.

Interconnected MOP like those observed in UHM-25 have been described by either treating them as cuboctahedra[86,87] or as rhombic cuboctahedra.[88,89] However, the treatment of the MOPs as rhombic cuboctahedra neglects the role of the copper paddle wheel as a 4-c node and leads to the description of an underlying 5-c net, whereas neither the linker nor the paddle wheel show this connectivity. Hence, Yaghi and O'Keeffe have proposed to treat such systems as interconnected cuboctahedra.[86] There are at least three ways to connect two neighboring cuboctahedra:

(a) In an arrangement where two faces of the cuboctahedra are pointing at each other.

(b) In an arrangement where the corners of the cuboctahedra are pointing at each other.

(c) In an arrangement where a corner of one cuboctahedron is pointing at the face of the neighboring cuboctahedron.

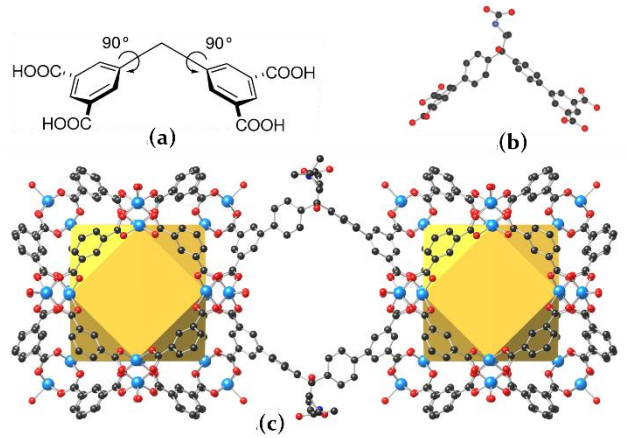

Figure 4. Interconnection of cuboctahedra in UHM-25-Val. a) Schematic representation of the conformation adopted by the linker in the MOF. b) Three-dimensional representation of the linker. c) Neighboring MOP in UHM-25-Val are connected only via their faces but not via their corners.

Three nets that represent interconnected cuboctahedra have been documented by Yaghi and O'Keeffe.[86] In the **zmj** net, the arrangements (a) and (b) can be observed. In the **zhc** net the arrangements (a) and (c) are found. The **ucp** net of UHM-25 constitutes the simplest of these nets as only the arrangement of type (a) is present. Figure 4 shows the connectivity of neighboring cuboctahedra in UHM-25-Val.

Apart from different synthesis conditions (solvent, temperature), the structural properties of the linkers are particularly decisive for the formation of certain topologies. The **zmj**, **zhc**, and **ucp** topologies have been observed only, if V-shaped tetracarboxylate linkers are used to build MOFs. Each of the three types of connections (a–c) between the cuboctahedra requires the linker to adopt a certain conformation with respect to the isophthalate moieties. These conformations can be discerned by the torsion of the isophthalate moieties and are depicted in Figure 5. First, for a connection in manner (a), the isophthalates adopt a non-coplanar conformation where both isophthalates adopt torsion angles of 90°. Second, for a connection in manner (b), the isophthalates are in a coplanar orientation (torsion angles: 0°, 0°). Third, for a connection in manner (c) the isophthalates are in a non-coplanar orientation and adopt torsion angles of 0° and 90°, respectively.

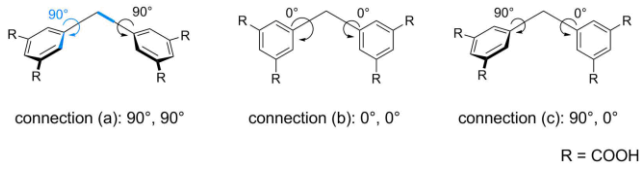

Figure 5. Three conformations of V-shaped diisophthalate linkers that are required to interconnect MOP in a specific manner (see text); the conformations are distinguished by the torsion angle of the two isophthalate moieties, which is exemplarily highlighted in blue for connection type (a).

The fact that only type (a) connections are observed in the UHM-25 MOFs suggests that the necessary conformation of the isophthalates is preferred over the other two arrangements shown in Figure 5. This is possibly due to the hydroxy and chiral substituents at the tetrahedral carbon atom, inducing the observed conformation of the biphenyl systems.

The realization of MOFs with **ucp** topology is important with respect of the so-called *principle of minimal transitivity*. It states that the vast majority of MOFs and other related network compounds build structures based on nets that have a minimum number of different kind of vertices p and for a particular value of p a minimum number of different kind of edges q.[84] **zhc** (the net of PCN-12, ref. 90) is one of the most complicated nets that has been

realized so far, with $pq = 89$, and **zmj** (realized for instance in ref. 88) – being still a fairly complicated 4-nodal net – has the transitivity $pq = 45$. Both nets have been known for a relatively long time. However, the simplest net consisting of two differently coordinated species (3-c and 4-c) to connect cuboctahedra consistent with the principle of minimal transitivity ($pq = 22$), namely **ucp**, was realized only now.

Figure 6 depicts the natural tiling of the **ucp** net, which aids the understanding of the arrangement of the pores in UHM-25. However, it should be noted that this representation neglects the size relationship between the different pore types.

There are four distinct types of pores in MOFs of the UHM-25 series: First, the spherical volume inside the MOP with a diameter of ~12 Å which is represented as a yellow tile in Figure 6. The space framed by the "concave" sides of the linker forms a second set of pores, represented by the red tiles, which are located on the edges of the unit cell. These pores connect the MOP to each other. The "convex" sides of the linker form an octapodal pore at the center of the unit cell. These pores include the chiral substituents and are represented by blue tiles. A fourth pore type connects the pores with the chiral substituents to each other. The centroids of these pores coincide with those of the faces of the unit cell. This type of pore is represented as a green tile in Figure 6. The voids in the UHM-25 MOFs form a three-dimensional, interconnected pore system.

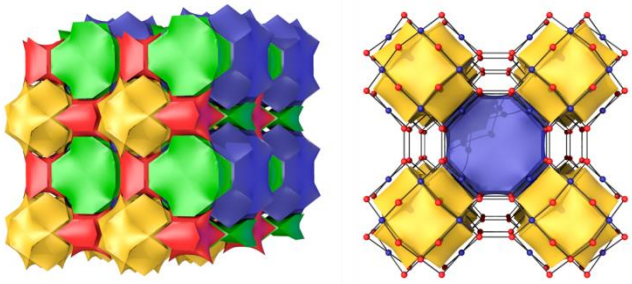

Figure 6. Topological representation of UHM-25 as a natural tiling and the underlying **ucp** net. Left: 2 × 2 × 2 supercell of the tiling. Right: Part of the **ucp** net that is carried by its respective tiling; four-coordinated nodes are blue, three-coordinated nodes are red. Only two of the four types of tiles are shown for clarity. Yellow tiles represent the MOP, blue tiles represent the pore space in which the amino acid substituents are located.

Porosity and thermal analysis. In order to evaluate the porosity of the UHM-25 MOF series, nitrogen physisorption measurements were carried out. Activation of the MOFs involved a stepwise solvent-exchange with DMF, THF, and amyl acetate followed by supercritical drying with carbon dioxide. Even when applying this mild activation procedure, satisfying specific surface areas could not be inferred in all cases, indicating a limited robustness of the framework with respect to complete solvent removal. However, a specific surface area of S_{BET} = 1922 $m^2 g^{-1}$ (calculated from the adsorption branch and in the relative pressure interval from 0.009 to 0.020) and a micropore volume of V_{pore} = 1.00 $cm^3 g^{-1}$ (calculated at $p/p_0 = 0.20$) could be achieved for UHM-25-Val-Boc (for a full overview of the values for all samples, see SI), compared to a theoretical value of $S_{theor.}$ = 2200 $m^2 g^{-1}$ of a completely activated sample evaluated with the Atom Surface and Volume tool of the Accelrys Materials Studio suite.[91] The nitrogen physisorption measurement for UHM-25-Val-Boc shows a typical type I(b) isotherm[92] and is depicted in Figure 7.

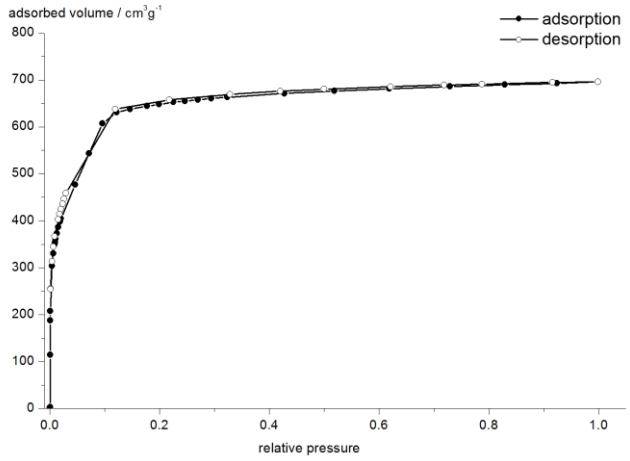

Figure 7. Nitrogen physisorption isotherm of activated UHM-25-Val-Boc measured at 77 K.

As a general trend, it can be observed that the MOFs bearing an *N*-Boc protecting group show higher surface areas than their non-protected counterparts.

In order to assess the thermal stability of the UHM-25 MOFs we carried out thermogravimetric analysis in an Ar/O_2 atmosphere (80:20) coupled with mass spectrometry (TGA-MS). Thermal stability might be an importance aspect considering potential catalysis reactions under non-ambient conditions. After evaporation of remaining solvents (water/THF, $m/z = 18/42$) up to temperatures of approx. 220 °C the decomposition of the unprotected UHM-25 MOFs proceeds in two consecutive steps between ~ 250–440 °C (see SI for details). The cleavage of the Boc group from the respective *N*-protected MOFs occurs in a well-separated step that can be clearly distinguished from the combustion of the MOF itself and takes place at temperatures at around 180 °C, which can be monitored by the characteristic isobutene cleavage product ($m/z = 56$).

As shown by Telfer and coworkers, it should be principally possible to cleave *N*-Boc protecting groups within MOFs by heating the material to ~ 150 °C.[70] Therefore, we applied similar conditions to evaluate a possible *N*-Boc deprotection for the UHM-25 MOFs. Unfortunately, and in contrast to Telfer's experience, thermal deprotection of the *N*-Boc protected UHM-25 MOFs resulted in X-ray amorphous materials. However, please note, in order to obtain deprotected MOFs, it was not necessary to perform the synthesis with the *N*-Boc protected linkers. Unlike in Telfer's findings, it was no problem to synthesize the MOFs from the ammonium salts of the linker molecules **6a–c**. We did not observe any implications on the synthesis of the UHM-25 MOFs out of linkers containing unprotected amino groups.

Post-synthetic modification and catalysis. Aiming at realizing systems for heterogeneous, asymmetric applications, we incorporated (a) a 1,3-oxazolidin-2-one (the so-called Evans auxiliary[93,94]) and (b) a α,α-diaryl prolinol residue into the organic building unit of the UHM-25 MOF platform. In the case of the oxazolidinone, we want to establish a chiral auxiliary system in the solid state. Consequently, we have performed a post-synthetic modification that constitutes the first step of a typical reaction sequence commonly associated with the Evans auxiliary in stereoselective

synthesis. Further reaction steps, such as the formation of a chiral enolate are still under investigation.

In order to use such a MOF as a solid-state Evans auxiliary, the NH function of the carbamate has to be acylated. Post-synthetic acylation is a straightforward process for MOF-bound amines.[18,34] However, amides are far less nucleophilic and thus less reactive than amines and require activation before acylation can take place.

Common procedures to obtain acylated oxazolidinones in homogeneous syntheses such as deprotonation of the NH function with *n*-butyllithium and the subsequent reaction with an acyl electrophile or using lithium chloride as an acylation catalyst failed to provide an acylated derivative of UHM-25-Val-Evans. However, the acylation of the MOF-bound oxazolidinone was achieved by applying a procedure that uses 4-(dimethylamino)pyridine (DMAP) as a catalyst, see Scheme 4.[95,96] DMAP reacts with propionic anhydride and the resulting reagent serves as an efficient acyl donor to the oxazolidinone in UHM-25-Val-Evans to give UHM-25-Val-Evans-PSM. Stirring the reaction mixture at room temperature led to a 37 % *N*-acylation of the MOF-bound carbamate functional groups within 24 hours. Extending the reaction to 72 h led to conversion rates of 90 %. To determine the conversion rates, the MOF samples were digested after modification using diluted hydrochloric acid to isolate the mixture of the linker Evans-Val-ta and its *N*-acylated derivative, whose relative proportions were estimated by ^{1}H NMR spectroscopy (for a detailed description, see SI). To assert the chemical stability of the MOF, powder X-ray diffractograms of the MOF before and after the PSM were compared and show retention of the crystal structure of the MOF (see SI for details).

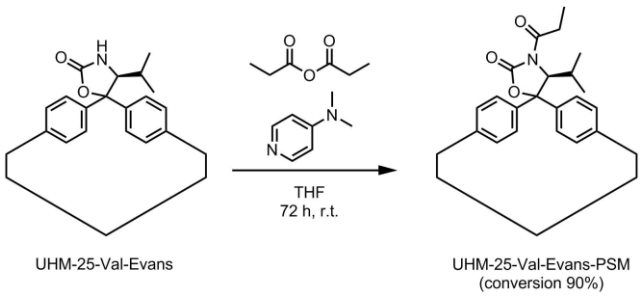

Scheme 4. Post-synthetic acylation of UHM-25-Val-Evans with propionic acid anhydride gave UHM-25-Val-Evans-PSM (the diamond shape indicates the framework host of the chiral substituent).

Apart from the post-synthetic modification of UHM-25-Val-Evans, we also wanted to assess the use of a UHM-25 MOF in heterogeneous catalysis. We chose UHM-25-Pro, which includes a α,α-diaryl prolinol motif. This group is known as a homogeneous catalyst in aldol additions but has, to the best of our knowledge, not been included in a MOF so far.[76,97] As a catalysis test reaction system we chose the self-directed aldol reaction of acetaldehyde. This reaction is depicted in Scheme 5.

To prepare the MOF for the reaction, UHM-25-Pro was pretreated with THF, then with dichloromethane to replace the solvent of the MOF synthesis with the solvent of the catalysis. Thus treated UHM-25-Pro was suspended in dichloromethane and acetaldehyde was added to yield a 10 % (*v/v*) solution. The reaction mixture was stirred at room temperature for five days. Afterwards, UHM-25-Pro was removed by filtration and the filtrate was treated with methanol and Amberlyst 15. This procedure converted aldehyde **9** to the respective acetal **10**. The conversion of the aldehyde facilitates work-up and analysis by decreasing the volatility of **9.** After evaporation of methanol, the resulting liquid reaction product that was obtained with a yield of 45 % was analyzed with enantioselective GC/MS (H_2 as the carrier gas, heptakis-(2,3-di-*O*-methyl-6-*O*-*tert*-butyldimethylsilyl)-β-cyclodextrin on fused silica as the stationary phase, see SI for details). The total ion chromatogram (TIC) of this separation is shown in Figure 8. The absolute configuration of the reaction products was assigned according to literature.[96] The (*R*)-enantiomer is the main product and the enantiomeric ratio was determined to be 70:30.

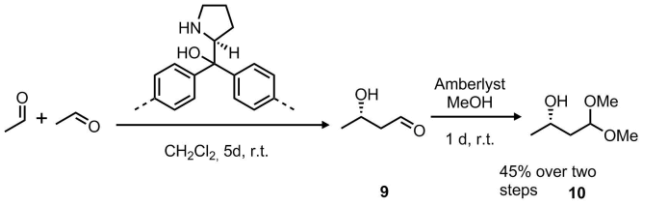

Scheme 5. Self-directed aldol addition of acetaldehyde catalyzed by UHM-25-Pro and the subsequent conversion of 3-hydroxybutanal (9) to 1,1-dimethoxy-3-hydroxybutane (10).

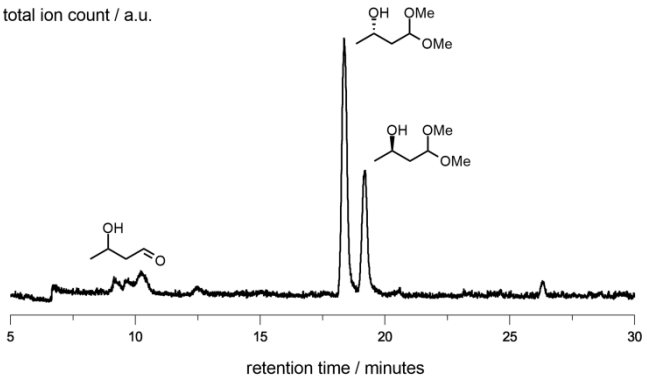

Figure 8. Total ion chromatogram from an enantioselective GC/MS separation of the product from the self-directed aldol addition of acetaldehyde catalyzed by UHM-25-Pro and the subsequent conversion to **10**.

To estimate the performance of the heterogeneous reaction established with UHM-25-Pro, an experiment using (*S*)-1,1-diphenyl-2-pyrrolidinemethanol was performed under homogeneous reaction conditions. This led to the aldol product with an enantiomeric ratio of 75:25, being slightly higher than the ratio of the respective heterogeneous reaction.

The induction of stereochemical information in the reaction product proves the chiral nature and the catalytic activity of UHM-25-Pro. The observed enantiomeric ratios are lower than those for homogeneous systems documented in the literature.[97] However, these reactions are highly dependent on the nature of the α,α-diaryl substituents on the prolinol catalyst as well as solvent effects. Bulky, electron-withdrawing α-aryls may stabilize important reaction intermediates.[98] Therefore, we see room for improvement for the heterogeneous catalyst system of UHM-25-Pro by introducing substituents that significantly reduce the electron density on the geminal aromatic rings.

CONCLUSIONS

Amino acids are a valuable source of chiral information in the synthesis of MOFs. The functional groups of the amino acids can be retained during the steps necessary to construct a MOF. The results presented above prove the success of a strategy based on chiral pool starting materials to synthesize a series of isoreticular, porous materials with accessible chiral substituents. The integrated functionality in the materials can be used in a stereoselective reaction. Compounds from the UHM-25 series are – to the best of our knowledge – the first MOFs with a catalytically active α,α-diaryl prolinol unit. Furthermore, UHM-25-Val-Evans provides an *accessible* Evans auxiliary. In contrast to previously published MOFs in which the auxiliary is bound to the framework via the nitrogen atom,[69] the oxazolidinone moiety can be acylated in a post-synthetic modification reaction. This could potentially be utilized in stereoselective syntheses on solid supports.

Finally, the geometry of the linker molecule allows the formation of the simplest topology of interconnected cuboctahedral MOP (**ucp**), which can be regarded as a confirmation of the validity of the principle of minimal transitivity.

REFERENCES

(1) Branch, S. K.; Hutt, A. J. Regulatory Perspective on the Development of New Stereoisomeric Drugs. In *Drug Stereochemistry – Analytical Methods and Pharmacology*, third edition; Jóźwiak, K., Lough, W. J., Wainer, I. W., Eds.; Drugs and the Pharmaceutical Sciences Volume 211; informa healthcare: London, 2012; pp 240–273.

(2) Zhang, L.; Cui, L.; Luo, S.; Cheng, J.-P. Supported Asymmetric Organocatalysis. In *Green Techniques for Organic Synthesis and Medicinal Chemistry*; Zhang, W., Cue Jr., B. W., Eds.; John Wiley & Sons, Ltd: Chichester, 2012; pp 99–136.

(3) Heitbaum, M.; Glorius, F.; Escher, I. Asymmetric Heterogeneous Catalysis. *Angew. Chem. Int. Ed.* **2006**, *45*, 4732–4762.

(4) Suh, M. P.; Park, H. J.; Prasad, T. K.; Lim, D.-W. Hydrogen Storage in Metal–Organic Frameworks. *Chem. Rev.* **2012**, *112*, 782–835.

(5) Yan, Y.; Yang, S.; Blake, A. J.; Schröder, M. Studies on Metal–Organic Frameworks of Cu(II) with Isophthalate Linkers for Hydrogen Storage. *Acc. Chem. Res.* **2014**, *47*, 296–307.

(6) He, Y.; Zhou, W.; Qian, G.; Chen, B. Methane Storage in Metal–Organic Frameworks. *Chem. Soc. Rev.* **2014**, *43*, 5657–5678.

(7) Sumida, K.; Rogow, D. L.; Mason, J. A.; McDonald, T. M.; Bloch, E. D.; Herm, Z. R.; Bae, T.-H.; Long, J. R. Carbon Dioxide Capture in Metal–Organic Frameworks. *Chem. Rev.* **2012**, *112*, 724–781.

(8) Queen, W. L.; Hudson, M. R.; Bloch, E. D.; Mason, J. A.; Gonzalez, M. I.; Lee, J. S.; Gygi, D.; Howe, J. D.; Lee, K.; Darwish, T. A.; James, M.; Peterson, V. K.; Teat, S. J.; Smit, B.; Neaton, J. B.; Long, J. R.; Brown, C. M. Comprehensive Study of Carbon Dioxide Adsorption in the Metal–Organic Frameworks M_2(dobdc) (M = Mg, Mn, Fe, Co, Ni, Cu, Zn). *Chem. Sci.* **2014**, *5*, 4569–4581.

(9) Li, J.-R.; Sculley, J.; Zhou, H.-C. Metal–Organic Frameworks for Separations. *Chem. Rev.* **2012**, *112*, 869–932.

(10) Qiu, S.; Xue, M.; Zhu, G. Metal–Organic Framework Membranes: From Synthesis to Separation Application. *Chem. Soc. Rev.* **2014**, *43*, 6116–6140.

(11) Van de Voorde, B.; Bueken, B.; Denayer, J.; De Vos, D. Adsorptive Separation on Metal-Organic Frameworks in the Liquid Phase. *Chem. Soc. Rev.* **2014**, *43*, 5766–5788.

(12) Snurr, R. Q.; Hupp, J. T.; Nguyen, S. T. Prospects for Nanoporous Metal-Organic Materials in Advanced Separations Processes. *AIChE J.* **2004**, *50*, 1090–1095.

(13) Liu, J.; Chen, L.; Cui, H.; Zhang, J.; Zhang, L.; Su, C.-Y. Applications of Metal–Organic Frameworks in Heterogeneous Supramolecular Catalysis. *Chem. Soc. Rev.* **2014**, *43*, 6011–6061.

(14) Czaja, A. U.; Trukhan, N.; Müller, U. Industrial Applications of Metal–Organic Frameworks. *Chem. Soc. Rev.* **2009**, *38*, 1284–1293.

(15) Lee, J.; Farha, O. K.; Roberts, J.; Scheidt, K. A.; Nguyen, S. T.; Hupp, J. T. Metal–Organic Framework Materials as Catalysts. *Chem. Soc. Rev.* **2009**, *38*, 1450–1459.

ASSOCIATED CONTENT

Supporting Information. Experimental procedures and analytical data for the organic intermediates. experimental procedures, nitrogen physisorption isotherms and TGA-MS plots of the UHM-25 MOFs, crystallographic information of UHM-25-Ala-Boc and UHM-25-Pro, TIC and MS traces from enantio-GC/MS of the enantioselective reaction. This material is available free of charge via the Internet at http://pubs.acs.org. Crystallographic information is deposited at the Cambridge Crystallographic Data Centre (CCDC) for UHM-25-Ala-Boc (CCDC No. 1415562) and UHM-25-Pro (CCDC No. 1415563).

AUTHOR INFORMATION

Corresponding Author

*E-mail: froeba@chemie.uni-hamburg.de. Phone: +49-40-42838-3101. Fax: +49-40-42838-6348.

ACKNOWLEDGEMENT

The authors thank Prof. Dr. Ulrich Behrens for helpful discussions regarding the crystal structure determination of the UHM-25 MOFs. Figures 3 and 4 were produced with VESTA.[99]

(16) Corma, A.; García, H.; Llabrés i Xamena, F. X. Engineering Metal Organic Frameworks for Heterogeneous Catalysis. *Chem. Rev.* **2010**, *110*, 4606–4655.

(17) Gascon, J.; Corma, A.; Kapteijn, F.; Llabrés i Xamena, F. X. Metal Organic Framework Catalysis: Quo Vadis? *ACS Catal.* **2014**, *4*, 361–378.

(18) Ma, L.; Abney, C.; Lin, W. Enantioselective Catalysis with Homochiral Metal-Organic Frameworks. *Chem. Soc. Rev.* **2009**, *38*, 1248–1256.

(19) Nickerl, G.; Henschel, A.; Grünker, R.; Gedrich, K.; Kaskel, S. Chiral Metal-Organic Frameworks and Their Application in Asymmetric Catalysis and Stereoselective Separation. *Chem. Ing. Tech.* **2011**, *83*, 90–103.

(20) Wang, C.; Zheng, M.; Lin, W. Asymmetric Catalysis with Chiral Porous Metal–Organic Frameworks: Critical Issues. *J. Phys. Chem. Lett.* **2011**, *2*, 1701–1709.

(21) Falkowski, J. M.; Liu, S.; Lin, W. Metal-Organic Frameworks as Single-Site Solid Catalysts for Asymmetric Reactions. *Isr. J. Chem.* **2012**, *52*, 591–603.

(22) Ma, L.; Falkowski, J. M.; Abney, C.; Lin, W. A Series of Isoreticular Chiral Metal–Organic Frameworks as a Tunable Platform for Asymmetric Catalysis. *Nat. Chem.* **2010**, *2*, 838–846.

(23) Falkowski, J. M.; Sawano, T.; Zhang, T.; Tsun, G.; Chen, Y.; Lockard, J. V.; Lin, W. Privileged Phosphine-Based Metal-Organic Frameworks for Broad-Scope Asymmetric Catalysis. *J. Am. Chem. Soc.* **2014**, *136*, 5213–5216.

(24) Mo, K.; Yang, Y.; Cui, Y. A. Homochiral Metal–Organic Framework as an Effective Asymmetric Catalyst for Cyanohydrin Synthesis. *J. Am. Chem. Soc.* **2014**, *136*, 1746–1749.

(25) Regati, S.; He, Y.; Thimmaiah, M.; Li, P.; Xiang, S.; Chen, B.; Zhao, J. C.-G. Enantioselective Ring-Opening of *Meso*-Epoxides by Aromatic Amines Catalyzed by a Homochiral Metal–Organic Framework. *Chem. Commun.* **2013**, *49*, 9836–9838.

(26) Xuan, W.; Ye, C.; Zhang, M.; Chen, Z.; Cui, Y. A Chiral Porous Metallosalan-Organic Framework Containing Titanium-Oxo Clusters for Enantioselective Catalytic Sulfoxidation. *Chem. Sci.* **2013**, *4*, 3154–3159.

(27) Cho, S.-H.; Ma, B.; Nguyen, S. T.; Hupp, J. T.; Albrecht-Schmitt, T. A Metal–Organic Framework Material That Functions as an Enantioselective Catalyst for Olefin Epoxidation. *Chem. Commun.* **2006**, 2563–2565.

(28) Song, F.; Wang, C.; Lin, W. A Chiral Metal-Organic Framework for Sequential Asymmetric Catalysis. *Chem. Commun.* **2011**, *47*, 8256–8258.

(29) Jing, X.; He, C.; Dong, D.; Yang, L.; Duan, C. Homochiral Crystallization of Metal–Organic Silver Frameworks: Asymmetric [3+2] Cycloaddition of an Azomethine Ylide. *Angew. Chem. Int. Ed.* **2012**, *51*, 10127–10131.

(30) Banerjee, M.; Das, S.; Yoon, M.; Choi, H. J.; Hyun, M. H.; Park, S. M.; Seo, G.; Kim, K. Postsynthetic Modification Switches an Achiral Framework to Catalytically Active Homochiral Metal–Organic Porous Materials. *J. Am. Chem. Soc.* **2009**, *131*, 7524–7525.

(31) Morris, R. E. Ionothermal Synthesis—Ionic Liquids as Functional Solvents in the Preparation of Crystalline Materials. *Chem. Commun.* **2009**, 2990–2998.

(32) Morris, R. E.; Bu, X. H. Induction of Chiral Porous Solids Containing Only Achiral Building Blocks. *Nat. Chem.* **2010**, *2*, 353–361.

(33) Bradshaw, D.; Prior, T. J.; Cussen, E. J.; Claridge, J. B.; Rosseinsky, M. J. Permanent Microporosity and Enantioselective Sorption in a Chiral Open Framework. *J. Am. Chem. Soc.* **2004**, 6106–6114.

(34) Hao, X.-R.; Wang, X.-L.; Qin, C.; Su, Z.-M.; Wang, E.-B.; Lan, Y.-Q.; Shao, K.-Z. A 3D Chiral Nanoporous Coordination Framework Consisting of Homochiral Nanotubes Assembled from Octuple Helices. *Chem. Commun.* **2007**, 4629–4622.

(35) Bisht, K. K.; Suresh, E. Spontaneous Resolution to Absolute Chiral Induction: Pseudo-Kagomé Type Homochiral Zn(II)/Co(II) Coordination Polymers with Achiral Precursors. *J. Am. Chem. Soc.* **2013**, *135*, 15690–15693.

(36) Zhao, X.; He, H.; Dai, F.; Sun, D.; Ke, Y. Supramolecular Isomerism in Honeycomb Metal–Organic Frameworks Driven by CH···π Interactions: Homochiral Crystallization from an Achiral Ligand through Chiral Inducement. *Inorg. Chem.* **2010**, *49*, 8650–8652.

(37) Dang, D.; Wu, P.; He, C.; Xie, Z.; Duan, C. Homochiral Metal–Organic Frameworks for Heterogeneous Asymmetric Catalysis. *J. Am. Chem. Soc.* **2010**, *132*, 14321–14323.

(38) Gil-Hernández, B.; Höppe, H. A.; Vieth, J. K.; Sanchiz, J.; Janiak, C. Spontaneous Resolution Upon Crystallization of Chiral La(III) and Gd(III) MOFs from Achiral Dihydroxymalonate. *Chem. Commun.* **2010**, *46*, 8270–8272.

(39) Dybtsev, D. N.; Nuzhdin, A. L.; Chun, H.; Bryliakov, K. P.; Talsi, E. P.; Fedin, V. P.; Kim, K. A Homochiral Metal–Organic Material with Permanent Porosity, Enantioselective Sorption Properties, and Catalytic Activity. *Angew. Chem. Int. Ed.* **2006**, *45*, 916–920.

(40) Dybtsev, D. N.; Yutkin, M. P.; Samsonenko, D. G.; Fedin, V. P.; Nuzhdin, A. L.; Bezrukov, A. A.; Bryliakov, K. P.; Talsi, E. P.; Belosludov, R. V; Mizuseki, H.; Kawazoe, Y.; Subbotin, O. S.; Belosludov, R. V. Modular, Homochiral, Porous Coordination Polymers: Rational Design, Enantioselective Guest Exchange Sorption and Ab Initio Calculations of Host–Guest Interactions. *Chem. Eur. J.* **2010**, *16*, 10348–10356.

(41) Ingleson, M. J.; Bacsa, J.; Rosseinsky, M. J. Homochiral H-Bonded Proline Based Metal Organic Frameworks. *Chem. Commun.* **2007**, 3036–3038.

(42) Livage, C.; Guillou, N.; Rabu, P.; Pattison, P.; Marrot, J.; Férey, G. Bulk Homochirality of a 3-D Inorganic Framework: Ligand Control of Inorganic Network Chirality. *Chem. Commun.* **2009**, 4551–4553.

(43) Ingleson, M. J.; Barrio, J. P.; Bacsa, J.; Dickinson, C.; Park, H.; Rosseinsky, M. J. Generation of a Solid Brønsted Acid Site in a Chiral Framework. *Chem. Commun.* **2008**, 1287–1289.

(44) Kaczorowski, T.; Justyniak, I.; Lipińska, T.; Lipkowski, J.; Lewiński, J. Metal Complexes of Cinchonine as Chiral Building Blocks: A Strategy for the Construction of Nanotubular Architectures and Helical Coordination Polymers. *J. Am. Chem. Soc.* **2009**, *131*, 5393–5395.

(45) Hao, H.-Q.; Liu, W.-T.; Tan, W.; Lin, Z.; Tong, M.-L. Enantiopure and Racemic Sandwich-Like Networks with Dehydration, Readsorption, and Selective Guest-Exchange Phase Transformations. *Cryst. Growth Des.* **2009**, *9*, 457–465.

(46) Rood, J. A.; Noll, B. C.; Henderson, K. W. Homochiral Frameworks Derived from Magnesium, Zinc and Copper Salts of L-Tartaric Acid. *J. Solid State Chem.* **2010**, *183*, 270–276.

(47) Seo, J. S.; Whang, D.; Lee, H.; Jun, S. I.; Oh, J.; Jeon, Y. J.; Kim, K. A Homochiral Metal–Organic Porous Material for Enantioselective Separation and Catalysis. *Nature* **2000**, *404*, 982–986.

(48) Wu, C.-D.; Hu, A.; Zhang, L.; Lin, W. A Homochiral Porous Metal-Organic Framework for Highly Enantioselective Heterogeneous Asymmetric Catalysis. *J. Am. Chem. Soc.* **2005**, *127*, 8940–8941.

(49) Peng, Y.; Gong, T.; Zhang, K.; Lin, X.; Liu, Y.; Jiang, J.; Cui, Y. Engineering Chiral Porous Metal-Organic Frameworks for Enantioselective Adsorption and Separation. *Nat. Commun.* **2014**, *5*, 4406.

(50) Tanaka, K.; Oda, S.; Shiro, M. A Novel Chiral Porous Metal-Organic Framework: Asymmetric Ring Opening Reaction of Epoxide with Amine in the Chiral Open Space. *Chem. Commun.* **2008**, 820–822.

(51) Jeong, K. S.; Go, Y. B.; Shin, S. M.; Lee, S. J.; Kim, J.; Yaghi, O. M.; Jeong, N. Asymmetric Catalytic Reactions by NbO-Type Chiral Metal–Organic Frameworks. *Chem. Sci.* **2011**, *2*, 877–882.

(52) Gedrich, K.; Senkovska, I.; Baburin, I. A.; Mueller, U.; Trapp, O.; Kaskel, S. New Chiral and Flexible Metal–Organic Framework with a Bifunctional Spiro Linker and Zn_4O-Nodes. *Inorg. Chem.* **2010**, *49*, 4440–4446.

(53) Strutt, N. L.; Zhang, H.; Stoddart, J. F. Enantiopure Pillar[5]arene Active Domains Within a Homochiral Metal-Organic Framework. *Chem. Commun.* **2014**, *50*, 7455–7458.

(54) Evans, O. R.; Ngo, H. L.; Lin, W. Chiral Porous Solids Based on Lamellar Lanthanide Phosphonates. *J. Am. Chem. Soc.* **2001**, *123*, 10395–10396.

(55) Evans, O. R.; Manke, D. R.; Lin, W. Homochiral Metal-Organic Frameworks Based on Transition Metal Bisphosphonates. *Chem. Mater.* **2002**, *14*, 3866–3874.

(56) Wu, C.-D.; Lin, W. Heterogeneous Asymmetric Catalysis with Homochiral Metal-Organic Frameworks: Network-Structure-Dependent Catalytic Activity. *Angew. Chem. Int. Ed.* **2007**, *46*, 1075–1078.

(57) Ong, T. T.; Kavuru, P.; Nguyen, T.; Cantwell, R.; Wojtas, Ł.; Zaworotko, M. J. 2:1 Cocrystals of Homochiral and Achiral Amino Acid Zwitterions with Li^+ Salts: Water-Stable Zeolitic and Diamondoid Metal-Organic Materials. *J. Am. Chem. Soc.* **2011**, *133*, 9224–9227.

(58) Zhang, J.; Yao, Y.-G.; Bu, X. Comparative Study of Homochiral and Racemic Chiral Metal-Organic Frameworks Built from Camphoric Acid. *Chem. Mater.* **2007**, *19*, 5083–5089.

(59) Rood, J.; Noll, B.; Henderson, K. A Homochiral Metal-Organic Framework with Amino-Functionalized Pores. *Main Gr. Chem.* **2009**, *8*, 237–250.

(60) Liang, X.-Q.; Li, D.-P.; Zhou, X.-H.; Sui, Y.; Li, Y.-Z.; Zuo, J.-L.; You, X.-Z. Metal–Organic Coordination Polymers Generated from Chiral Camphoric Acid and Flexible Ligands with Different Spacer Lengths: Syntheses, Structures, and Properties. *Cryst. Growth Des.* **2009**, *9*, 4872–4883.

(61) Zhao, X.; Wong, M.; Mao, C.; Trieu, T. X.; Zhang, J.; Feng, P.; Bu, X. Size-Selective Crystallization of Homochiral Camphorate Metal–Organic Frameworks for Lanthanide Separation. *J. Am. Chem. Soc.* **2014**, *136*, 12572–12575.

(62) Anokhina, E. V; Jacobson, A. J. $[Ni_2O(L\text{-}Asp)(H_2O)_2]\cdot 4H_2O$: A Homochiral 1D Helical Chain Hybrid Compound with Extended Ni–O–Ni Bonding. *J. Am. Chem. Soc.* **2004**, *126*, 3044–3045.

(63) Vaidhyanathan, R.; Bradshaw, D.; Rebilly, J.-N.; Barrio, J. P.; Gould, J. A.; Berry, N. G.; Rosseinsky, M. J. A Family of Nanoporous Materials Based on an Amino Acid Backbone. *Angew. Chem. Int. Ed.* **2006**, *45*, 6495–6499.

(64) Perez Barrio, J.; Rebilly, J.-N.; Carter, B.; Bradshaw, D.; Bacsa, J.; Ganin, A. Y.; Park, H.; Trewin, A.; Vaidhyanathan, R.; Cooper, A. I.; Warren, J. E.; Rosseinsky, M. J. Control of Porosity Geometry in Amino Acid Derived Nanoporous Materials. *Chem. Eur. J.* **2008**, *14*, 4521–4532.

(65) Yang, X.-L.; Xie, M.-H.; Zou, C.; Sun, F.-F.; Wu, C.-D. A Series of Metal–Organic Coordination Polymers Containing Multiple Chiral Centers. *CrystEngComm* **2011**, *13*, 1570–1579.

(66) Sreenivasulu, B.; Vittal, J. J. Helix inside a Helix: Encapsulation of Hydrogen-Bonded Water Molecules in a Staircase Coordination Polymer. *Angew. Chem. Int. Ed.* **2004**, *43*, 5769–5772.

(67) Rossin, A.; Di Credico, B.; Giambastiani, G.; Peruzzini, M.; Pescitelli, G.; Reginato, G.; Borfecchia, E.; Gianolio, D.; Lamberti, C.; Bordiga, S. Synthesis, Characterization and CO_2 Uptake of a Chiral Co(II) Metal–Organic Framework Containing a Thiazolidine-Based Spacer. *J. Mater. Chem.* **2012**, *22*, 10335–10344.

(68) Banerjee, S.; Adarsh, N. N.; Dastidar, P. An Unprecedented All Helical 3D Network and a Rarely Observed Non-Interpenetrated Octahedral Network in Homochiral Cu(II) MOFs: Effect of Steric Bulk and π–π Stacking Interactions of the Ligand Backbone. *CrystEngComm* **2009**, *11*, 746–749.

(69) Gedrich, K.; Heitbaum, M.; Notzon, A.; Senkovska, I.; Fröhlich, R.; Getzschmann, J.; Mueller, U.; Glorius, F.; Kaskel, S. A Family of Chiral Metal–Organic Frameworks. *Chem. Eur. J.* **2011**, *17*, 2099–2106.

(70) Lun, D. J.; Waterhouse, G. I. N.; Telfer, S. G. A General Thermolabile Protecting Group Strategy for Organocatalytic Metal–Organic Frameworks. *J. Am. Chem. Soc.* **2011**, *133*, 5806–5809.

(71) Kutzscher, C.; Hoffmann, H. C.; Krause, S.; Stoeck, U.; Senkovska, I.; Brunner, E.; Kaskel, S. Proline Functionalization of the Mesoporous Metal–Organic Framework DUT-32. *Inorg. Chem.* **2015**, *54*, 1003–1009.

(72) Xu, Z.-X.; Tan, Y.-X.; Fu, H.-R.; Liu, J.; Zhang, J. Homochiral Metal–Organic Frameworks with Enantiopure Proline Units for the Catalytic Synthesis of β-Lactams. *Inorg. Chem.* **2014**, *53*, 12199–12204.

(73) Lili, L.; Xin, Z.; Shumin, R.; Ying, Y.; Xiaoping, D.; Jinsen, G.; Chunming, X.; Jing, H. Catalysis by Metal-Organic Frameworks: Proline and Gold Functionalized MOFs for the Aldol and Three-Component Coupling Reactions. *RSC Adv.* **2014**, *4*, 13093–13107.

(74) Canivet, J.; Farrusseng, D. Proline-Functionalized Metal–Organic Frameworks and Their Use in Asymmetric Catalysis: Pitfalls in the MOFs Rush. *RSC Adv.* **2015**, *5*, 11254–11256.

(75) Mukherjee, S.; Yang, J. W.; Hoffmann, S.; List, B. Asymmetric

Enamine Catalysis. *Chem. Rev.* **2007**, *107*, 5471–5569.

(76) Meninno, S.; Lattanzi, A. Asymmetric Organocatalysis Mediated by α,α-L-Diaryl Prolinols: Recent Advances. *Chem. Commun.* **2013**, *49*, 3821–3832.

(77) Marigo, M.; Wabnitz, T. C.; Fielenbach, D.; Jørgensen, K. A. Enantioselective Organocatalyzed α Sulfenylation of Aldehydes. *Angew. Chem. Int. Ed.* **2005**, *44*, 794–797.

(78) Hayashi, Y.; Gotoh, H.; Hayashi, T.; Shoji, M. Diphenylprolinol Silyl Ethers as Efficient Organocatalysts for the Asymmetric Michael Reaction of Aldehydes and Nitroalkenes. *Angew. Chem. Int. Ed.* **2005**, *44*, 4212–4215.

(79) Blaser, H. U. The Chiral Pool as a Source of Enantioselective Catalysts and Auxiliaries. *Chem. Rev.* **1992**, *92*, 935–952.

(80) Hiyoshizo, K.; Sasakura, N. Proline-Related Secondary Amine Catalysts and Applications. In *Comprehensive Enantioselective Organocatalysis*; Dalko, P. I., Ed.; Wiley-VCH: Weinheim, 2013; pp 1–31.

(81) List, B.; Lerner, R. A.; Barbas III, C. F. Proline-Catalyzed Direct Asymmetric Aldol Reactions. *J. Am. Chem. Soc.* **2000**, *122*, 2395–2396.

(82) Hoffmann, F.; Hühnerfuss, H.; Stine, K. J. Temperature Dependence of Chiral Discrimination in Langmuir Monolayers of N-Acyl Amino Acids as Inferred from II/A Measurements and Infrared Reflection–Absorption Spectroscopy. *Langmuir* **1998**, *14*, 4525–4534.

(83) These MOP are well-known structural motifs on their own (ref. 84) or in extended frameworks (ref. 85).

(84) Li, M.; Li, D.; O'Keeffe, M.; Yaghi, O. M. Topological Analysis of Metal–Organic Frameworks with Polytopic Linkers and/or Multiple Building Units and the Minimal Transitivity Principle. *Chem. Rev.* **2014**, *114*, 1343–1370.

(85) Blatov, V. A.; Shevchenko, A. P.; Proserpio, D. M. Applied Topological Analysis of Crystal Structures with the Program Package ToposPro. *Cryst. Growth Des.* **2014**, *14*, 3576–3586.

(86) O'Keeffe, M.; Yaghi, O. M. Deconstructing the Crystal Structures of Metal–Organic Frameworks and Related Materials into Their Underlying Nets. *Chem. Rev.* **2012**, *112*, 675–702.

(87) Liu, X.; Park, M.; Hong, S.; Oh, M.; Yoon, J. W.; Chang, J.-S.; Lah, M. S. A Twofold Interpenetrating Porous Metal–Organic Framework with High Hydrothermal Stability: Structure and Gas Sorption Behavior. *Inorg. Chem.* **2009**, *48*, 11507–11509.

(88) Perry IV, J. J.; Kravtsov, V. C.; McManus, G. J.; Zaworotko, M. J. Bottom Up Synthesis That Does Not Start at the Bottom: Quadruple Covalent Cross-Linking of Nanoscale Faceted Polyhedra. *J. Am. Chem. Soc.* **2007**, *129*, 10076–10077.

(89) Perry IV, J. J.; Perman, J. A.; Zaworotko, M. J. Design and Synthesis of Metal–Organic Frameworks Using Metal–Organic Polyhedra as Supermolecular Building Blocks. *Chem. Soc. Rev.* **2009**, *38*, 1400–1417.

(90) Wang, X.-S.; Ma, S.; Forster, P. M.; Yuan, D.; Eckert, J.; López, J. J.; Murphy, B. J.; Parise, J. B.; Zhou, H.-C. Enhancing H_2 Uptake by "Close-Packing" Alignment of Open Copper Sites in Metal–Organic Frameworks. *Angew. Chem. Int. Ed.* **2008**, *47*, 7263–7266.

(91) Accelrys, San Diego, CA, USA 2010.

(92) Thommes, M.; Kaneko, K.; Neimark, A. V.; Olivier, J. P.; Rodriguez-Reinoso, F.; Rouquerol, J.; Sing, K. S. W. Physisorption of Gases, With Special Reference to the Evaluation of Surface Area and Pore Size Distribution (IUPAC Technical Report). *Pure Appl. Chem.* **2015**, *87*, 1051–1069.

(93) Evans, D. A. Studies in Asymmetric Synthesis. The Development of Practical Chiral Enolate Synthons. *Aldrichim. Acta* **1982**, *15*, 23–32.

(94) Evans, D. A.; Ennis, M. D.; Mathre, D. J. Asymmetric Alkylation Reactions of Chiral Imide Enolates. A Practical Approach to the Enantioselective Synthesis of *α*-Substituted Carboxylic Acid Derivatives. *J. Am. Chem. Soc.* **1982**, *104*, 1737–1739.

(95) Ager, D. J.; Allen, D. R.; Schaad, D. R. Simple and Efficient *N*-Acylation Reactions of Chiral Oxazolidine Auxiliaries. *Synthesis* **1996**, 1283–1285.

(96) Xu, S.; Held, I.; Kempf, B.; Mayr, H.; Steglich, W.; Zipse, H. The DMAP-Catalyzed Acetylation of Alcohols—A Mechanistic Study (DMAP=4-(Dimethylamino)pyridine). *Chem. Eur. J.* **2005**, *11*, 4751–4757.

(97) Hayashi, Y.; Samanta, S.; Itoh, T.; Ishikawa, H. Asymmetric, Catalytic, and Direct Self-Aldol Reaction of Acetaldehyde Catalyzed by Diarylprolinol. *Org. Lett.* **2008**, *10*, 5581–5583.

(98) Schmid, M. B.; Zeitler, K.; Gschwind, R. M. Formation and Stability of Prolinol and Prolinol Ether Enamines by NMR: Delicate Selectivity and Reactivity Balances and Parasitic Equilibria. *J. Am. Chem. Soc.* **2011**, *133*, 7065–7074.

(99) Momma, K.; Izumi, F. VESTA 3 for Three-Dimensional Visualization of Crystal, Volumetric and Morphology Data. *J. Appl. Cryst.* **2011**, *44*, 1272–1276.

TOC graphic